Three-Dimensional Chemical Mapping with a Confocal XRF Setup

ARTICLE *in* ANALYTICAL CHEMISTRY · FEBRUARY 2013

Impact Factor: 5.64 · DOI: 10.1021/ac303749b · Source: PubMed

5 AUTHORS, INCLUDING:

Lars Lühl
Technische Universität Berlin
10 PUBLICATIONS **189** CITATIONS
SEE PROFILE

Ioanna Mantouvalou
Technische Universität Berlin
23 PUBLICATIONS **251** CITATIONS
SEE PROFILE

Carla Vogt
Leibniz Universität Hannover
78 PUBLICATIONS **2,562** CITATIONS
SEE PROFILE

Birgit Kanngießer
Technische Universität Berlin
94 PUBLICATIONS **1,133** CITATIONS
SEE PROFILE

analytical chemistry

Article

pubs.acs.org/ac

Three-Dimensional Chemical Mapping with a Confocal XRF Setup

Lars Lühl,*[,†] Ioanna Mantouvalou,[†] Ina Schaumann,[‡,§] Carla Vogt,[‡] and Birgit Kanngießer[†]

[†]Technische Universität Berlin, Berlin, Germany

[‡]Leibnitz Universität Hannover, Hannover, Germany

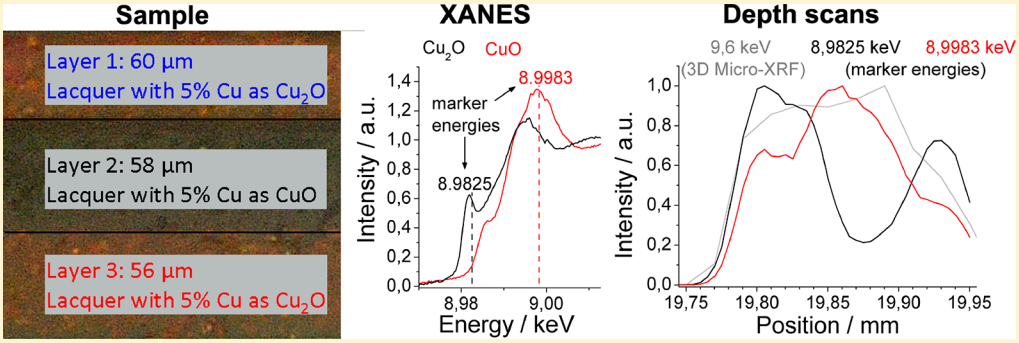

ABSTRACT: A new approach for the nondestructive reconstruction of stratified systems with constant elemental composition but with varying chemical compounds has been developed. The procedure is based on depth scans with a confocal X-ray fluorescence setup at certain energies near absorption edges. These so-called marker energies, where XAFS signals of the involved chemical compounds differ significantly, can also be used to uncover the chemical composition and its topology. A prominent field of application is homogeneous material that is degraded due to chemical reactions like oxidation or reduction. A procedure for the semiquantitative reconstruction of stratified material by means of depth scans at marker energies is elaborated and validated and a three-dimensional mapping is presented.

The reconstruction of depth scans with a confocal setup at certain energies near absorption edges fills the gap between conventional 3D Micro X-ray fluorescence analysis (3D Micro-XRF) and 3D Micro X-ray absorption fine structure spectroscopy (3D Micro-XAFS). The confocal setup has been developed to facilitate a three-dimensional elemental analysis.[1−3] A detailed description of the setup is given by Malzer et al.[4] and Mantouvalou et al.[5] It uses one polycapillary halflens in the excitation channel to focus the radiation and one in the detection channel in front of the detector to restrict its field of view. The overlap of both foci creates a probing volume where the detected signal originates from (Figure 1).

Up to now the confocal setup is either used to investigate the elemental distribution into depth for stratified material[6] or 3-dimensionally for small objects[7] or to investigate different chemical states of an analyte in layers of stratified material.[8] The reconstruction procedure for 3D Micro-XRF of stratified material reveals thicknesses and compositions of layered specimen with varying elemental compositions in the layers.[6] 3D Micro-XAFS on the other hand, with known thicknesses and elemental compositions of layers, reveals the chemical compound of the analyte in the layers.[8] Until now a reconstruction of layer thicknesses is not possible for a constant elemental composition but varying chemical compounds in the layers. This gap can be closed by the presented method of depth scans at certain energies near absorption edges.

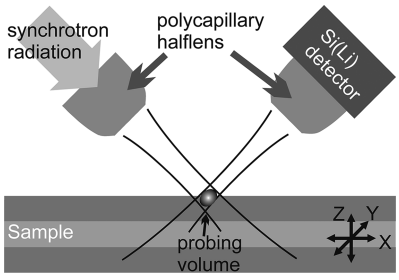

Figure 1. Sketch of the confocal setup for 3D Micro-XRF and 3D Micro-XAFS.

Lateral mapping of oxidation states with conventional geometry without a lens in front of the detector at marker energies was performed by several research groups in different fields. For example, mapping of Se-oxidation state in environmental science[9] or mapping of growth lines of mollusc shells near S K-edge[10] and Cr-oxidation states of mammalian cells[11] in biology. All applications are restricted to lateral resolution while depth resolved mapping of chemical states for thick objects was not performed until now. Three-dimensional chemical mapping of Ni of small (a few μm) battery particles was performed by Meirer et al. with 3D transmission X-ray microscopy (TXM) XANES.[12] TXM XANES is performed in transmission mode and thus not applicable for thick samples.

Received: December 23, 2012
Accepted: February 27, 2013
Published: February 27, 2013

We present a reconstruction procedure and its validation for layered samples with constant elemental composition but varying chemical compounds in the layers that is based on the definition of marker energies as energies with a significant difference in the XAFS intensity of the involved chemical compounds. The procedure is based on the reconstruction procedure of 3D Micro-XRF[5] and is adapted to the use of marker energies. In addition, marker energies are suitable to uncover the topology of such samples. Topology is meant here to indicate the chemical compounds and their distribution (location) within the analyzed volume.

The validation of the reconstruction procedure and topology analysis is shown with the help of self-produced reference material containing copper(I)- (Cu_2O) and copper(II)-oxide (CuO). Copper was chosen as analyte because it is widely used in cultural heritage objects, where such layered systems are typical for corrosion processes. During corrosion the chemical compounds of an analyte do change, but the elemental composition may stay unchanged. So far, 3D nondestructive analysis of the topology of corrosion products within thick samples, i.e., XAFS in fluorescence mode, has not yet been made possible.

THEORY AND ALGORITHMS

The reconstruction algorithm for depth scans at marker energies is based on both the quantification procedure for 3D Micro-XRF[5] and the reconstruction procedure for 3D Micro-XAFS spectra.[8] First the intensity equations for both calibration of the setup and reconstruction of the layered specimen are presented, followed by a description of an enhanced calibration method and the reconstruction procedure. The calibration procedure for 3D Micro-XAFS was developed further in order to obtain exact values for both calibration parameters close to the absorption edge. The reconstruction procedure is then elaborated for the layered specimen with constant elemental distribution but varying chemical compounds of the analyte.

Intensity Equations. The reconstruction procedure of depth scans at marker energies relies on an expression of the primary fluorescence intensity ($I_l(x,E_0)$) as a function of the probing depth (x) and exciting energy (E_0). Equation 1 is the basic equation for a single homogeneous layer l with layer boundaries at d_l and d_{l-1} and the thickness $D_l = d_l - d_{l-1}$. The intensity of a specific X-ray emission line can be written as

$$I_l(x, E_0) = I_0 \eta \sigma_F \rho \cdot e^{(-\bar{\mu}_{lin} x)} \cdot e^{(\bar{\mu}_{lin}\sigma_x)^2/2} \left[\operatorname{erf}\left(\frac{d_l + \bar{\mu}_{lin}\sigma_x^2 - x}{\sqrt{2}\,\sigma_x} \right) - \operatorname{erf}\left(\frac{d_{l-1} + \bar{\mu}_{lin}\sigma_x^2 - x}{\sqrt{2}\,\sigma_x} \right) \right] \quad (1)$$

where I_0 is the intensity of the X-rays impinging onto the specimen with the energy E_0. The integral sensitivity η and the width of the probing volume σ_x in the scanning direction are the calibration parameters characterizing the confocal setup. Both parameters depend on the excitation and fluorescence energies.[5,8] The production cross section σ_F accounts for all atomic processes leading to the emission of the X-ray fluorescence line:

$$\sigma_F = (\tau \cdot j)_{XAFS} \cdot \omega \cdot g \quad (2)$$

where ω is the fluorescence yield and g represents the transition property. The product of the photoionization cross section τ and the jump factor j represents the undistorted XAFS signal and is labeled with XAFS in order to distinguish it from atomic values. In general fundamental parameters taking into account XAFS oscillations of the chemical compound of the analyte are called XAFS parameters.

$\bar{\mu}_{lin}$ is the so-called effective linear mass attenuation coefficient, which comprises the attenuation of the excitation and fluorescence intensities, including the geometry of the setup. The excitation part of the effective linear mass attenuation coefficient contains as well the product of the photoionization cross section and the jump factor $(\tau \cdot j)_{XAFS}$.[8]

For a stratified specimen the absorption of upper layers must be taken into account. The detected overall intensity ($I(x,E_0)$) for an n-layered system can be written as the sum of all n layers' contribution:[5]

$$I(x, E_0) = \sum_{l=1}^{n} \prod_{k=1}^{l-1} e^{(-\mu_{lin,k} D_k)} I_l(x, E_0) \quad (3)$$

Enhanced Calibration Procedure. For calibration eq 1 or 3 has to be solved for the calibration parameters, the integral sensitivity η, and the width of the probing volume σ_x by means of reference material. This is carried out by least-squares fitting of depth scans.[5] In contrast to 3D Micro-XRF the confocal setup for 3D Micro-XAFS measurements and for depths scans at marker energies has to be calibrated for various excitation energies in the XAFS region.[8]

For an adequate calibration procedure, especially near the absorption edge, the atomic fundamental parameters listed in databases are not sufficient. Near the edge there can be significant differences between atomic and XAFS cross sections of the chemical compound.

This is emphasized in Figure 2, where the atomic (solid line) and XAFS (dashed line) photoionization cross sections of the copper K-edge are shown. The atomic photoionization cross section and jump factor are extracted from the Elam database.[13] The XAFS photoionization cross sections of the copper K-edge are determined by measuring a 2 μm thin copper foil in transmission mode and afterward the spectrum is normalized to the corresponding atomic values. The XAFS values of the photoionization cross section of the copper K-edge are about

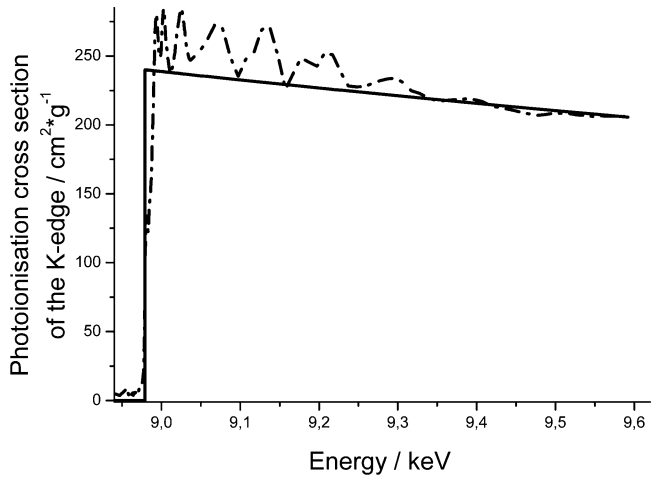

Figure 2. The atomic photoionization cross section of the copper K-edge (solid line) and the XAFS one for pure bulk copper (dashed line) are depicted.

dx.doi.org/10.1021/ac303749b | Anal. Chem. 2013, 85, 3682−3689

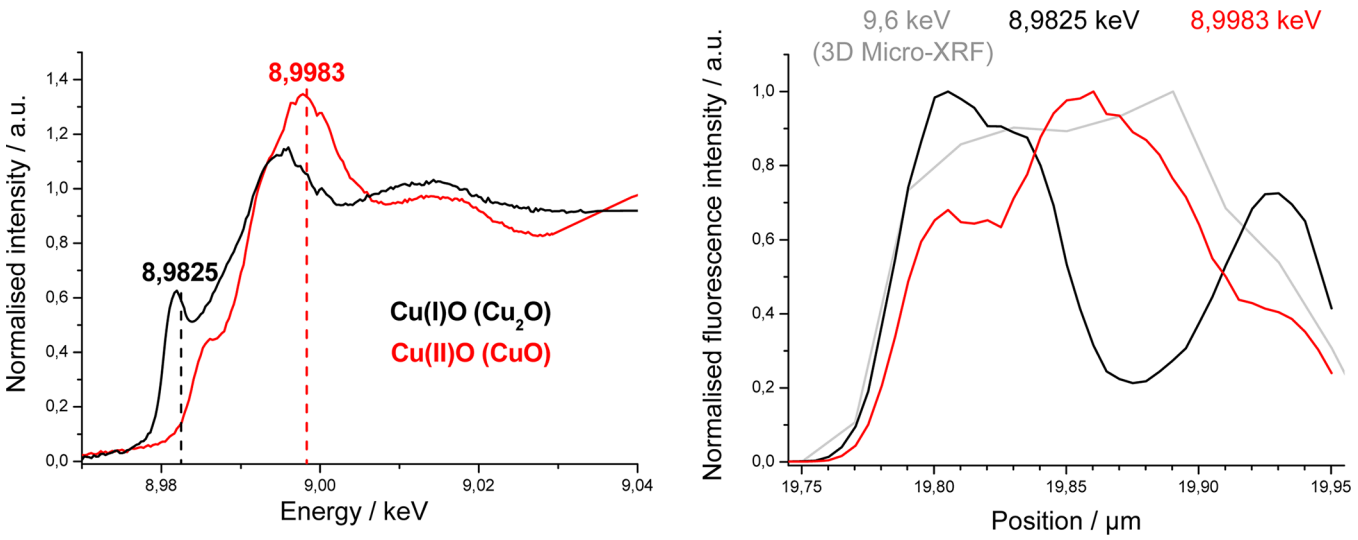

Figure 3. Left: XANES spectra of Cu(I)-oxide (black) and Cu(II)-oxide (red). The two characteristic marker energies are presented with vertical lines. Right: Depth scans at marker energies and at 9.6 keV (gray).

half the value of the corresponding atomic ones shortly after the absorption edge (compare also Figure 6, right). This difference renders the calibration procedure with listed atomic fundamental parameters in this region unreliable.

Hence, for an adequate calibration procedure it is necessary to know, besides the elemental composition and the density of the reference sample, the XAFS spectrum of the analyte in the chemical state existent in the reference sample as well. That means a thin or diluted sample suitable to measure in transmission mode without absorption effects should be available. Due to the availability of pure element thin foils with known chemical states, pure element standards are a good choice, except for very reactive elements.

For the calibration procedure the XAFS spectra of the reference samples are normalized to the corresponding atomic photoionization cross sections of the investigated edge. For energies at which depth scans for the calibration are performed, the XAFS photoionization cross sections of the investigated edge $(\tau \cdot j)_{\mathrm{XAFS}}$ can be extracted from the normalized XAFS spectra and used for the calibration procedure.

Reconstruction. To introduce our reconstruction algorithm, the main objectives are discussed by means of measured XAFS spectra and intensity depth profiles. Figure 3 on the left side shows X-ray absorption near edge spectroscopy (XANES) spectra of Cu(I)- and Cu(II)-oxides. Two energies are highlighted with vertical dashed lines at which significant differences of both XANES signals are present. At 8.9825 keV (black dashed line) the setup is more sensitive to Cu(I)-oxide than to Cu(II)-oxide whereas at 8.9983 keV (red dashed line) it is the other way around. These energies with a significant difference in the XANES intensity of the involved chemical compounds are called marker energies.

Scanning a stack of lacquer layers with constant copper concentration present as Cu(I)-oxide in the first and third layers and as Cu(II)-oxide in the layer in between leads to the normalized net peak intensity depth profiles of Figure 3, right. In black the depth profile detected for the marker energy 8.9825 keV is shown while 8.9983 keV is shown in red. At 8.9825 keV higher intensity for layers with Cu(I)-oxide is detected than for those with Cu(II)-oxide and at 8.9983 keV it is the other way around. With conventional 3D Micro-XRF with excitation energies far away from the absorption edge, where there is no difference in fundamental parameters for Cu(I)- and Cu(II)-oxide, the layers are not distinguishable as shown by the depth scan at 9.6 keV in gray.

Similar to 3D Micro-XRF the objective of semiquantitative evaluation of such depth profiles is to reconstruct layer thicknesses and to determine the composition of the chemical compounds of the analyte in the layers.[5] Adapting the reconstruction procedure of 3D Micro-XRF to depth scans at marker energies leads to challenges which are discussed in the following.

For the reconstruction of layers thicknesses and elemental compositions with excitation energies far above any absorption edge each detectable element corresponds to a certain fluorescence intensity. That means each detected net peak intensity can directly be ascribed to an element. In contrast, for depth scans at marker energies the fluorescence signal of only one element is detected for various chemical compounds. Thus, it is not possible to assign the detected fluorescence signal to the chemical compound of the analyte. Additionally in 3D Micro-XRF, different fluorescence energies exhibit different absorption properties.

For a unique solution of the system of equations, the number of depth scans at different marker energies to be chosen must be at least equal to the number of chemical compounds or additional information such as the overall elemental concentration of the analyte has to be known.

The adaption of the reconstruction process changes the simultaneous fitting of several depth profiles of different fluorescence energies detected for one excitation energy in 3D Micro-XRF into a simultaneous fitting of depth profiles of one fluorescence energy of the analyte at different excitation energies in 3D Micro-XANES.

For the reconstruction procedure the XANES spectra of the different chemical compositions have to be known in order to determine the real fundamental parameters near the absorption edge. They can either be determined by transmission measurements of references, which is the most precise solution, or for corrosion processes by 3D Micro-XANES at corroded and uncorroded positions.

dx.doi.org/10.1021/ac303749b | Anal. Chem. 2013, 85, 3682−3689

All involved XANES spectra have to be normalized for atomic values similar to the procedure used for pure copper in the calibration procedure (Figure 2) in order to extract the XANES photoionization cross sections of the investigated edge $(\tau \cdot j)_{XAFS}$ for various excitation energies. Afterward the XANES parameter can be extracted for all chemical compounds and marker energies directly. In Figure 4 the normalized spectra for

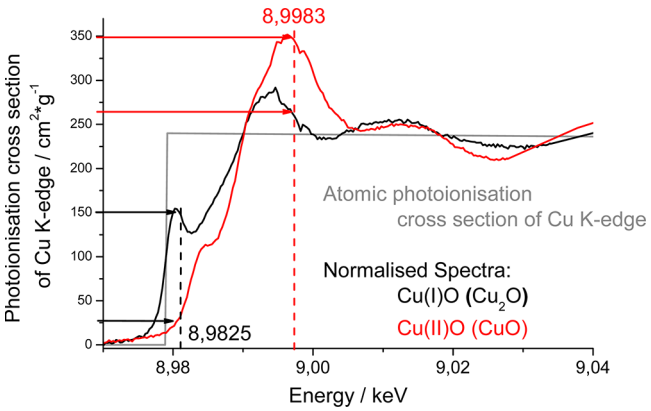

Figure 4. Atomic photoionization cross section of Cu K-edge and normalized XANES spectra of Cu(I)-oxide (black) and Cu(II)-oxide (red) with respect to atomic values. Marker energies (dashed vertical lines) and XANES photoionization cross sections for both chemical compounds at both marker energies (arrows).

Cu(I)- (black) and Cu(II)-oxide (red) are shown together with the atomic values (gray). The black arrows mark the cross sections of both chemical compounds for the marker energy of 8.9825 keV and the red ones for 8.9983 keV.

For reconstructing the system of an unknown sample, various parameters are inserted into eq 3: integral sensitivity η, width of the probing volume σ_x, and the extracted XANES photoionization cross sections of the investigated edge for all involved chemical compounds $(\tau \cdot j)_{XAFS}$ and marker energies. Initial values for elemental composition and thickness of each layer as well as number and succession of layers must be given in advance. Calculated values are compared and adapted to measured ones by varying the concentration of chemical compounds and layer thicknesses in a least-squares-fit algorithm. Depth scans of all marker energies are fitted simultaneously.

EXPERIMENTAL SECTION

The experimental validation of the reconstruction procedure for depth scans at marker energies was carried out at the μSpot beamline of Berlin's synchrotron radiation facility BESSY II.[14]

According to the data sheet of the polycapillary halflens in the excitation channel, it produces a spot size of about 30 μm $fwhm_E$ on the specimen for the energy region around the copper K-edge. The $fwhm_D$ of the polycapillary halflens of the detection channel is 18 μm in that energy region. After careful alignment to overlap both spots the width of the probing volume normal to the sample surface was determined by the calibration procedure to be $\sigma_x = (11.6 \pm 0.2)$ μm, this corresponds to a $fwhm_x$ of (27.3 ± 0.5) μm.

A seven-element Si(Li) detector was used, and the polycapillary halflens was placed in front of one of the crystals. A sufficient spectral resolution of the excitation radiation was provided by a Si (311) double crystal monochromator with an approximate energy resolution of $E/\Delta E \approx 25\,000$.

Calibration. For the calibration of the confocal setup, a thick pure copper standard and a 2 μm thin copper foil were used. The thick pure copper standard was used for the calibration yielding the integral sensitivity η scaled with a conversion constant k and the width of the probing volume normal to the specimen's surface σ_x. Both parameters have to be determined by depth scans at energies around the copper K-edge which is used in this work. The conversion constant k relates the incoming flux (Φ_0) to the measured current (I_0) of a calibrated ionization chamber according to the following equation: $\Phi_0 = kI_0$.

For a calibration at excitation energies near absorption edges XANES cross sections differ from listed atomic ones. To determine the XANES values, the thin copper foil was used to measure a XANES spectrum of the reference material in transmission mode, hence without distortion due to absorption effects. The XANES spectrum was normalized to atomic values so that XANES photoionization cross sections of investigated edges for various excitation energies can be extracted and used for the calibration (Figure 2).

Experimentally, depth scans at seven energies close to the copper K-edge (8.98, 9.03, 9.04, 9.14, 9.30, 9.45, and 9.60 keV) were performed. The step size into depth was 5 μm and the acquisition time varied between 10 and 60 s depending on excitation energy and ring current.

For each depth scan the calibration parameters, η and σ_x, were determined. The results of the calibration are shown and discussed in the next section.

Reference Material. For validation, an ideal stratified reference material would be a light matrix containing a specific transition metal in various chemical compounds and distributed homogeneously in layers. To demonstrate that conventional 3D Micro-XRF is not sufficient for such cases, the elemental composition of the layers should be the same. Suitable layered reference material was not available commercially. Therefore, appropriate reference material for validation was manufactured by Ina Schaumann of the analytical research group of the Leibniz Universität Hannover.[15]

The stratified reference material was produced with UV-cured lacquer as matrix containing about 5% of copper as Cu(I)-oxide or Cu(II)-oxide. A sketch of the sample can be seen in Figure 5.

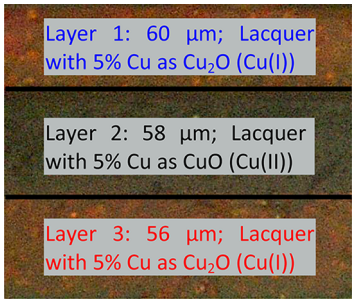

Figure 5. Sketch of the multilayered structure of reference sample used for validation.

In total, 90 depth scans were performed at each marker energy (8.9825 and 8.9983 keV). A quadrate of 0.4×0.4 mm^2 was screened with 81 (9×9) depth scans in lateral distances of 50 μm. For a 3-dimensional overview of the sample, a step width into depth of 20 μm was sufficient. Additionally, 9 depth scans at both excitation energies were performed with a step

dx.doi.org/10.1021/ac303749b | Anal. Chem. 2013, 85, 3682−3689

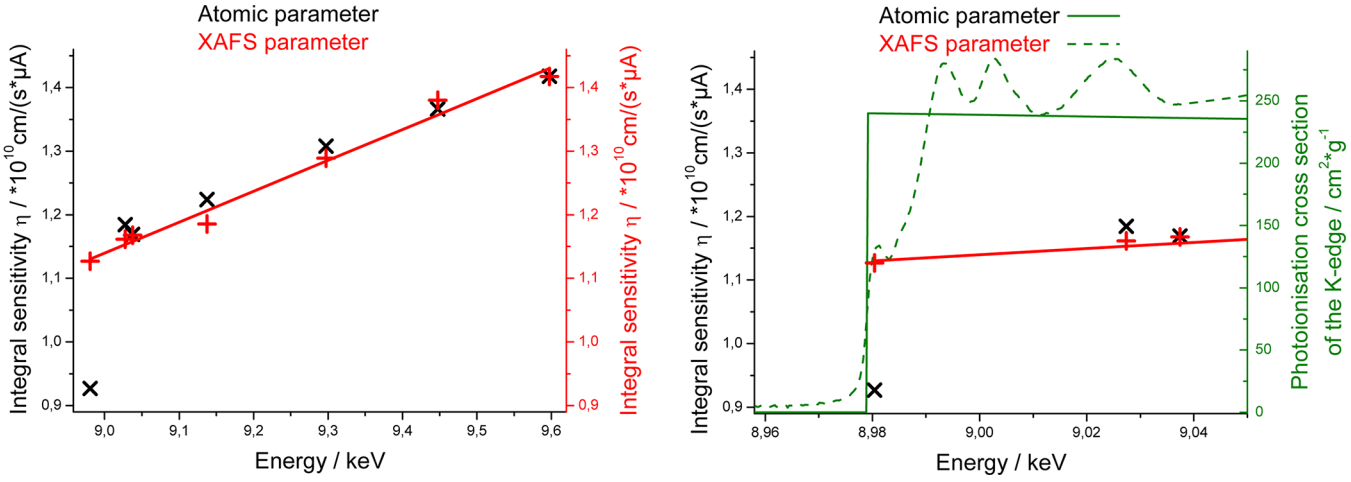

Figure 6. Left: Calculated integral sensitivity η using atomic parameters (black crosses) and XAFS ones (red plusses). Linear fit of the calculated integral sensitivity η for XAFS parameters (red solid line). Right: Cutout region of the absorption edge with plotted atomic (green solid) and XANES (green dashed) photoionization cross sections of the copper K-edge.

width into depth of 5 μm. The depth scans with smaller step sizes were used for reconstruction of layer thicknesses and determination of amount of Cu(I)- and Cu(II)-oxide. The acquisition time for each step was 20 s, which accumulates to about 20 min for one depth scan with smaller step sizes and to about 35 min for a volume of 9 depth scans with larger step sizes.

RESULTS

In this section, calibration results, layered specimen reconstruction, and visualization of the topology by 3D-mapping are presented. The results of the presented enhanced calibration procedure are compared with a calibration procedure using atomic parameters instead of XANES ones as presented for the reconstruction of 3D Micro-XAFS.[8] Furthermore, the result of the validation of the reconstruction procedure is shown for depth scans of the reference sample. At the end, an example for rendering the topology of an unknown sample is presented for the reference sample at the marker energy of 8.9825 keV.

Enhanced Calibration. Figures 6 and 7 show the results of the calibration procedure for seven excitation energies (8.98, 9.03, 9.04, 9.14, 9.30, 9.45, and 9.60 keV, respectively). The deduced integral sensitivity η is plotted in Figure 6. Using atomic parameters during calibration leads to black crosses, whereas XANES parameters are represented by red plusses.

The cutout region for the first three excitation energies on the right side clarifies the influence of the used fundamental parameters to the resulting integral sensitivity η. At 8.98 keV the atomic value of the photoionization cross section of the copper K-edge is about twice as high as the XANES one. That leads to a calculated integrated sensitivity which is 18% smaller as calculated with XANES parameters. For the second excitation energy of 9.03 keV it is the other way around but the difference is only 2%. And for the third energy of 9.04 keV, where the atomic and XANES values are quite similar, there is no difference in the calculated integral sensitivity.

The linear fit of the results calculated with XANES fundamental parameters is shown as a red line. The general increase of η with increasing energy is due to an increasing transmission of the lens in the excitation channel in the screened energy region.[16,17] The differences of the linear fits using atomic fundamental parameters (not shown) and XANES

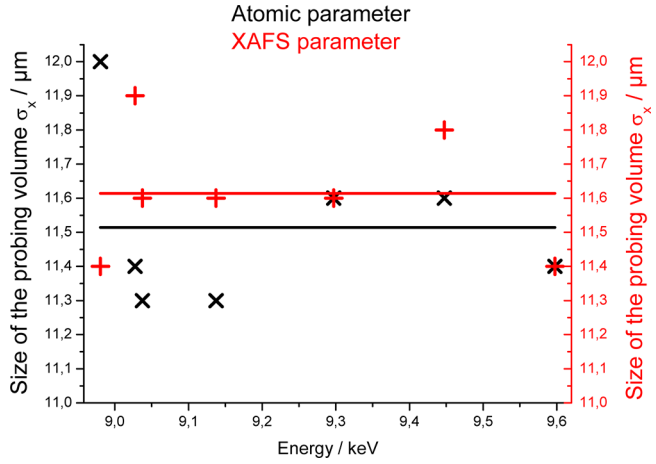

Figure 7. Calculated width of the probing volume σ_x using atomic parameters (black crosses) and XAFS ones (red plusses). Mean value of the width of the probing volume σ_x is depicted for XAFS (red line) and atomic parameters (black line).

ones (red line) reaches at maximum 10% in the scanned XANES region. For other elements the influence of atomic fundamental parameters used for the calibration process might be even higher.

Figure 7 shows the calculation results for the width of the probing volume σ_x. The results calculated with atomic fundamental parameters are marked as black crosses while those calculated with XAFS ones are marked as red plusses. The widths of the probing volume calculated with atomic fundamental parameters are up to 0.5 μm smaller than those calculated with XAFS parameters except for the first excitation energy (8.98 keV; 0.6 μm bigger). The general behavior of the width of the probing volume in the scanned energy region is constant with statistical variations. Hence, a mean value gives the best approximation. The mean value where atomic parameters were used is plotted as a black line and for XAFS ones as a red line. The difference of the mean values for the width of the probing volume calculated with atomic fundamental parameters and XAFS ones is less than 2%.

Reconstruction. Figure 8 shows the result of the simultaneous fit of eq 3 for two depth scans at both marker

dx.doi.org/10.1021/ac303749b | Anal. Chem. 2013, 85, 3682−3689

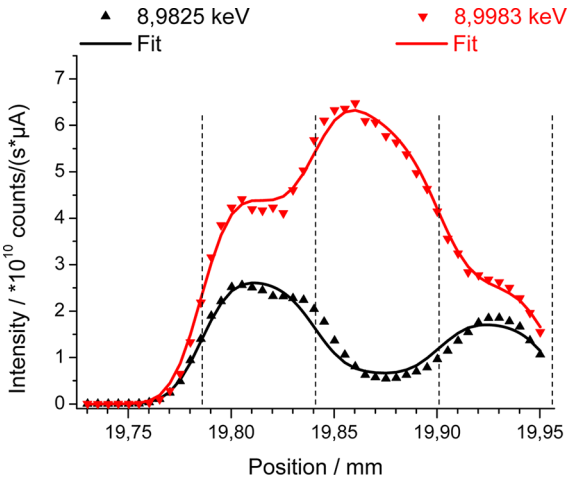

Figure 8. Depth scans (dots) at marker energies 8.9825 (black) and 8.9983 keV (red) and corresponding fits (solid curves). The borders of layers are shown as vertical dashed lines.

energies. The dots represent the measurements: black for marker energy of 8.9825 keV and red for 8.9983 keV. Fitting the measured depth scans with the help of the XANES photoionization cross sections of the copper K-edge extracted from Figure 4 led to the solid curves. The dashed vertical lines indicate the determined borders of the layers.

Table 1 lists the results of the reconstruction (left) and the corresponding values determined by independent methods (right). We determined the layer thicknesses by optical microscope and the copper concentrations in the layers by ICP-OES. Behind the reconstructed values (in parentheses) the differences to the corresponding values determined by independent methods are given as a percentage deviation.

As can be seen by the values in parentheses, layers thicknesses can be reconstructed within a maximum error of less than 10%. This is similar to the uncertainty for values of reconstructed thicknesses with 3D Micro-XRF.

For the reconstructed concentrations we distinguish between Cu(I)- and Cu(II)-oxide specimens. The concentration of copper present as Cu(I)-oxide (layers 1 and 3) is determined within an uncertainty of 14%. This is in the range of the accuracy of reconstruction with 3D Micro-XRF[6] but will not be achievable for all possible variations of the chemical copper compounds. For smaller differences in XANES signals of the chemical compounds at marker energies, uncertainties are expected to be higher.

The uncertainty for Cu(II)-oxide is located in a higher range of about 40%. In contrast to Cu(I)-oxide (Cu_2O) the Cu(II)-oxide (CuO) nanopowder agglomerates to particle sizes of up to 20 μm before dispersion, which could be shown on SEM images of the powders.[15] With static light scattering much smaller particle sizes of around 200 nm were measured in the lacquer after dispersion. For the static light measurements the lacquer had to be diluted with ethanol, which may influence the particle size. However, it got clear that the particle sizes in the lacquer are in the nanometer range after dispersion. Possibly, reagglomeration could occur while preparing and curing the layers. Particle sizes in the range of the width of the probing volume can falsify the determined results. Thus, the increased copper concentration determined for the second layer can be due to agglomerated particles or an inhomogeneous distribution in the scanned region.

Topology. For a three-dimensional scan at the marker energy of 8.9825 keV, the detected copper K_α signal normalized to the incoming flux and the acquisition time is plotted in Figure 9. On the left side the crossing of a plane parallel to surface (**YZ**) and planes perpendicular to that (**XZ** and **XY**) are plotted together and on the right side these planes are plotted separately with a slightly enhanced (planes **XZ** and **XY**) or reduced contrast (plane **YZ**). Bright or dark regions correspond respectively to high or low detected intensity.

As one can see in Figure 9 (right on the top) the signal is homogeneously distributed in the plane parallel to the surface. The detected intensity for the planes into depth (**XZ** and **XY**) rises when the probing volume hits the first layer. Although the copper concentration of all layers is nearly the same, it decreases when the probing volume intersects with the second layer due to less sensitivity of Cu(II)-oxide at the marker energy of 8.9825 keV than for Cu(I)-oxide (Figure 4) and then it rises again for the third layer.

This example shows the possibility to uncover the topology of different chemical compounds of unknown samples nondestructively by 3-dimensional mapping at marker energies.

DISCUSSION AND PERSPECTIVE

For a layered specimen with constant elemental distribution but alternating chemical compounds in the layers a reconstruction procedure by means of depth scans at marker energies has been developed and validated. The validation was carried out with a self-produced stratified reference sample containing about 5% Cu(I)-oxide in the first and the third layer and Cu(II)-oxide in the second layer.

The validation showed that reconstruction of a layered specimen by means of marker energies is able to reconstruct layers with alternating chemical copper compounds in the layers. The uncertainties in thicknesses and elemental compositions of reconstructed layers are comparable to 3D Micro-XRF. As in 3D Micro-XRF the uncertainties for real objects are expected to be higher due to diffuse interlayers.

Table 1. Layer Thicknesses and Amounts of Copper as Cu(I)- and Cu(II)-Oxides As Reconstructed by Present Method (Left) and As Measured by Independent Methods (Right)[a]

	reconstructed			determined by independent methods		
		Cu/wt%			Cu/wt%	
	thickness/μm	as Cu(I)O	as Cu(II)O	thickness/μm	as Cu(I)O	as Cu(II)O
layer 1	55 (8%)	4.6 (6%)	−0.1	60	4.9	0
layer 2	60 (3%)	0. 1	6.4 (39%)	58	0	4.6
layer 3	55 (2%)	4.2 (14%)	0.2	56	4.9	0

[a]In parentheses are the percentage deviations to the values determined with optical microscope for the thicknesses and with ICP-OES for the amount of copper.[15]

dx.doi.org/10.1021/ac303749b | Anal. Chem. 2013, 85, 3682−3689

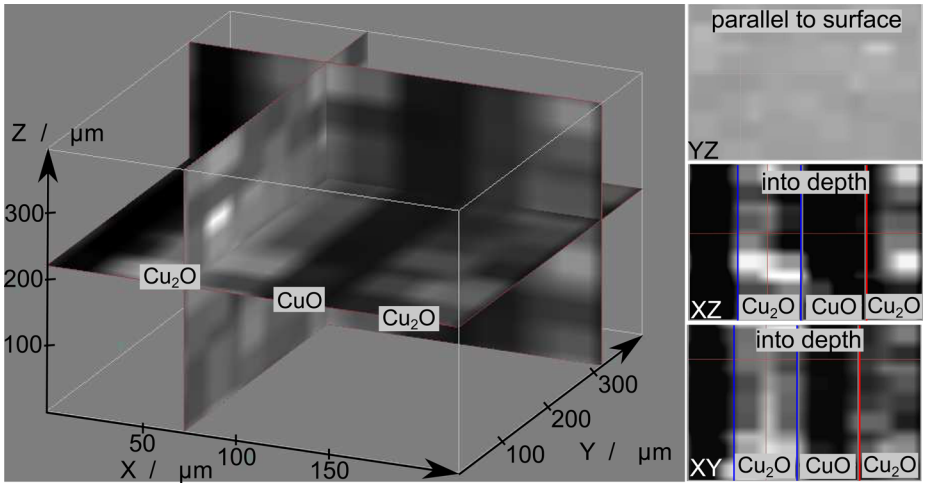

Figure 9. 3D Micro-XRF scan at marker energy 8.9825 keV. Brightest spot equals 7.6×10^{10} counts·s^{-1}·μA^{-1} and darkest spot 0. Left: Crossing of planes. Right (**YZ**, **XZ**, **XY**): Planes parallel to surface, **YZ** plane; vertical, **XZ** plane; and horizontal, **XY** plane.

In principle, the reconstruction procedure is applicable for different mixtures of chemical compounds in the layers. For example, a layered specimen with 80% of Cu(I)-oxide and 20% of Cu(II)-oxide in the first layer and 20% of Cu(I)-oxide and 80% of Cu(II)-oxide in the second layer should be reconstructable as well.

An enhanced calibration procedure using XAFS fundamental parameters has been developed and compared to the calibration procedure using listed atomic fundamental parameters. The enhanced calibration reveals calibration parameters which are more reliable especially in the energy range near the absorption edge.

For the reference sample a three-dimensional scan at one marker energy was performed in order to show the possibility to uncover the topology of chemical compounds non-destructively.

For both, the reconstruction of the stratified material and uncovering the topology the XANES spectra of the involved chemical compositions have to be known. Thus, for a correct analysis the involved chemical compounds should be measured in transmission mode as a reference. For corrosion processes reconstructed 3D Micro-XANES spectra of original and corroded material can also be used.

We chose copper as analyte for the reference samples, because it is widely used in cultural heritage objects. For example, corrosion processes of copper green pigments in reverse glass paintings are not fully understood yet. If marker energies are definable, this method may help to investigate the topology of corrosion products by 3-dimensional mapping or to semiquantitatively determine the extent of corrosion into depth by reconstruction of depths scans at marker energies.

This method is applicable to a broad range of degradation processes in cultural heritage such as iron-gall inks on manuscripts or in material science such as alteration processes of battery material. For degradation processes in general a common problem for XRF is a constant detected intensity due to no or only small changes in the elemental composition.

Hence, this method might prove to be helpful in advising proper conservation interventions and in material science investigations such as understanding alteration processes of batteries.

The method might be improved by a general study of the minimum needed contrast of the involved XANES spectra at the marker energies for an appropriate reconstruction of layer thicknesses or for revealing the topology of chemical compounds. It will help to decide the applicability case by case.

AUTHOR INFORMATION

Corresponding Author

*E-mail: Lars.Luehl@physik.tu-berlin.de.

Present Address

[§]German Institute of Rubber Technology, Hannover, Germany

Notes

The authors declare no competing financial interest.

ACKNOWLEDGMENTS

The authors acknowledge the support of Ivo Zizak from the μSpot beamline at BESSY during beamtimes.

REFERENCES

(1) Kanngiesser, B.; Malzer, W.; Reiche, I. *Nucl. Instrum. Methods Phys. Res., Sect. B* **2003**, *211*, 259−264.

(2) Vincze, L.; Vekemans, B.; Brenker, F.; Falkenberg, G.; Rickers, K.; Somogyi, A.; Kersten, M.; Adams, F. *Anal. Chem.* **2004**, *76*, 6786−6791.

(3) Tsuji, K.; Nakano, K.; Ding, ? *Spectrochim. Acta, Part B* **2007**, *62*, 549−553.

(4) Malzer, W.; Kanngiesser, B. *Spectrochim. Acta, Part B* **2005**, *60*, 1334−1341.

(5) Mantouvalou, I.; Malzer, W.; Schaumann, I.; Lühl, L.; Dargel, R.; Vogt, C.; Kanngiesser, B. *Anal. Chem.* **2008**, *80*, 819−826.

(6) Mantouvalou, I., Ph.D. Thesis, Universitätsbibliothek TU Berlin, 2009.

(7) Vekemenans, B.; Vince, L.; Brenker, F. E.; Adams, F. *J. Anal. At . Spectrom.* **2004**, *19*, 1302−1308.

(8) Lühl, L.; Mantouvalou, I.; Malzer, W.; Schaumann, I.; Vogt, C.; Hahn, O.; Kanngießer, B. *Anal. Chem.* **2012**, *84*, 1907−1914.

(9) Sutton, S. R.; Bajt, S.; Delaney, J.; Schulze, D.; Tokunaga, T. *Rev. Sci. Instrum.* **1995**, *66* (2), 1464−1467.

(10) Dauphin, Y.; Cuif, J. P.; Doucet, J.; Salomé, M.; Susini, J.; Williams, C. T. *Mar. Biol.* **2003**, *142*, 299−304.

(11) Ortega, R.; Fayard, B.; Salomé, M.; Devès, G.; Susini, J. *Chem. Res. Toxicol.* **2005**, *18*, 1512−1519.

(12) Meirer, F.; Cabana, J.; Lui, Y.; Metha, A.; Andrews, J. C.; Pianetta, P. *J. Synchrotron Radiat.* **2011**, *18*, 773−781.

(13) Elam, W. T.; Ravel, B. D.; Sieber, J. R. *Radiat. Phys. Chem.* **2002**, *63* (2), 121−128.

(14) Erko, A.; Zizak, I. *Spectrochimica Acta Part B* **2009**, *64*, 833−848.

(15) Schaumann, I., Ph.D. Thesis, Universitätsbibliothek Hannover, 2011.
(16) Malzer, W.; Kanngießer, B. *Spectrochim. Acta Part B* **2005**, *60*, 1334−1341.
(17) Wolff, T.; Mantouvalou, I.; Malzer, W.; Nissen, J.; Berger, D.; Zizak, I.; Sokaras, D.; Karydas, A.; Grlj, N.; Pelicon, P.; Schütz, R.; Zitnik, M.; Kanngießer, B. *J. Anal. At. Spectrom.* **2009**, *24*, 669−675.